

1 **Modern wolves trace their origin to a late Pleistocene expansion from Beringia**

2 Liisa Loog<sup>1,2,3\*</sup>, Olaf Thalmann<sup>4†</sup>, Mikkel-Holger S. Sinding<sup>5,6,7†</sup>, Verena J.  
3 Schuenemann<sup>8,9,10†</sup>, Angela Perri<sup>11</sup>, Mietje Germonpré<sup>12</sup>, Herve Bocherens<sup>9,13</sup>, Kelsey E.  
4 Witt<sup>14</sup>, Jose A. Samaniego Castruita<sup>5</sup>, Marcela S. Velasco<sup>5</sup>, Inge K. C. Lundstrøm<sup>5</sup>, Nathan  
5 Wales<sup>5</sup>, Gontran Sonet<sup>15</sup>, Laurent Frantz<sup>2</sup>, Hannes Schroeder<sup>5,16</sup>, Jane Budd<sup>17</sup>, Elodie-Laure  
6 Jimenez<sup>12</sup>, Sergey Fedorov<sup>18</sup>, Boris Gasparyan<sup>19</sup>, Andrew W. Kandel<sup>20</sup>, Martina Lázničková-  
7 Galetová<sup>21,22,23</sup>, Hannes Napierala<sup>24</sup>, Hans-Peter Uerpmann<sup>8</sup>, Pavel A. Nikolskiy<sup>25,26</sup>, Elena Y.  
8 Pavlova<sup>27,26</sup>, Vladimir V. Pitulko<sup>26</sup>, Karl-Heinz Herzig<sup>4,28</sup>, Ripan S. Malhi<sup>29</sup>, Eske  
9 Willerslev<sup>2,5,30</sup>, Anders J. Hansen<sup>5,7</sup>, Keith Dobney<sup>31,32,33</sup>, M. Thomas P. Gilbert<sup>5,34</sup>, Johannes  
10 Krause<sup>8,35</sup>, Greger Larson<sup>1\*</sup>, Anders Eriksson<sup>36,2\*</sup>, Andrea Manica<sup>2\*</sup>

11

12 \*Corresponding Authors: L.L. (liisaloog@gmail.com), G.L. (greger.larson@arch.ox.ac.uk),  
13 A.E. (anders.eriksson@kcl.ac.uk), A.M. (am315@cam.ac.uk)

14

15 †These authors contributed equally to this work

16

17 1 Palaeogenomics & Bio-Archaeology Research Network Research Laboratory for  
18 Archaeology and History of Art, University of Oxford, Dyson Perrins Building, South Parks  
19 Road, Oxford OX1 3QY, UK

20 2 Department of Zoology, University of Cambridge, Downing Street, Cambridge CB2 3EJ,  
21 UK

22 3 Manchester Institute of Biotechnology, School of Earth and Environmental Sciences,  
23 University of Manchester, Manchester, M1 7DN, UK

24 4 Department of Pediatric Gastroenterology and Metabolic Diseases, Poznan University of  
25 Medical Sciences, Szpitalna 27/33, 60-572 Poznan, Poland

26 5 Centre for GeoGenetics, Natural History Museum of Denmark, University of Copenhagen,  
27 Øster Voldgade 5-7, DK-1350 Copenhagen, Denmark

28 6 Natural History Museum, University of Oslo, P.O. Box 1172 Blindern, NO-0318 Oslo,  
29 Norway

30 7 The Qimmeq project, University of Greenland, Manutooq 1, PO Box 1061, 3905 Nuussuaq,  
31 Greenland

32 8 Institute for Archaeological Sciences, University of Tübingen, Rümelinstr. 23, 72070  
33 Tübingen, Germany

34 9 Senckenberg Centre for Human Evolution and Palaeoenvironment, University of Tübingen,  
35 72070 Tübingen, Germany

36 10 Institute of Evolutionary Medicine, University of Zurich, 8057 Zurich, Switzerland

- 1
- 2 11 Department of Human Evolution, Max Planck Institute for Evolutionary Anthropology,  
3 Deutscher Platz 6, 04103 Leipzig, Germany
- 4 12 OD Earth and History of Life, Royal Belgian Institute of Natural Sciences, Vautierstraat  
5 29, 1000 Brussels, Belgium
- 6 13 Department of Geosciences, Palaeobiology, University of Tübingen, Tübingen, Germany
- 7 14 School of Integrative Biology, University of Illinois at Urbana-Champaign, 109A  
8 Davenport Hall, 607 S. Mathews Avenue, Urbana IL 61801, USA
- 9 15 OD Taxonomy and Phylogeny, Royal Belgian Institute of Natural Sciences, Vautierstraat  
10 29, 1000 Brussels, Belgium
- 11 16 Faculty of Archaeology, Leiden University, Postbus 9514, 2300 RA Leiden, The  
12 Netherlands
- 13 17 Breeding Centre for Endangered Arabian Wildlife, PO Box 29922 Sharjah, United Arab  
14 Emirates
- 15 18 Mammoth Museum, Institute of Applied Ecology of the North of the North-Eastern  
16 Federal University, ul. Kulakovskogo 48, 677980 Yakutsk, Russia
- 17 19 National Academy of Sciences, Institute of Archaeology and Ethnography, Charents St.  
18 15, Yerevan 0025, Armenia
- 19 20 Heidelberg Academy of Sciences and Humanities: The Role of Culture in Early  
20 Expansions of Humans, Rümelinstr. 23, 72070 Tübingen, Germany
- 21 21 Departement of Anthropology, University of West Bohemia, Sedláčkova 15, 306 14  
22 Pilzen, Czech republic
- 23 22 Moravian museum, Zelný trh 6, 659 37 Brno, Czech republic
- 24 23 Hrdlička Museum of Man, Faculty of Science, Charles University, Viničná 1594/7,128 00  
25 Praha, Czech republic
- 26 24 Institute of Palaeoanatomy, Domestication Research and History of Veterinary Medicine,  
27 Ludwig-Maximilians-University Munich, Kaulbachstraße 37 III/313, D-80539 Munich,  
28 Germany
- 29 25 Geological Institute, Russian Academy of Sciences, 7 Pyzhevsky per., 119017 Moscow,  
30 Russia
- 31 26 Institute for Material Culture History, Russian Academy of Sciences, 18 Dvortsovaya nab.,  
32 St Petersburg 191186, Russia
- 33 27 Arctic and Antarctic Research Institute, 38 Bering St., St Petersburg 199397, Russia
- 34 28 Insitute of Biomedicine and Biocenter of Oulu, Medical Research Center and University  
35 Hospital, University of Oulu, Aapistie 5, 90220 Oulu University, Finland

- 1 29 Carl R. Woese Institute for Genomic Biology, University of Illinois at Urbana-Champaign,  
2 1206 W Gregory Dr., Urbana, Illinois 61820, USA
- 3 30 Wellcome Trust Sanger Institute, Hinxton, Cambridge CB10 1SA, UK
- 4 31 Department of Archaeology, Classics and Egyptology, University of Liverpool, 12-14  
5 Abercromby Square, Liverpool L69 7WZ, UK
- 6 32 Department of Archaeology, University of Aberdeen, St Mary's, Elphinstone Road,  
7 Aberdeen AB24 3UF, UK
- 8 33 Department of Archaeology, Simon Fraser University, Burnaby, B.C. V5A 1S6, 778-782-  
9 419, Canada
- 10 34 Norwegian University of Science and Technology, University Museum, N-7491  
11 Trondheim, Norway
- 12 35 Max Planck Institute for the Science of Human History, Khalaische Straße 10, 07745 Jena,  
13 Germany
- 14 36 Department of Medical & Molecular Genetics, King's College London, Guys Hospital,  
15 London SE1 9RT, UK
- 16

1 **ABSTRACT**

2 Grey wolves (*Canis lupus*) are one of the few large terrestrial carnivores that have maintained  
3 a wide geographic distribution across the Northern Hemisphere throughout the Pleistocene  
4 and Holocene. Recent genetic studies have suggested that, despite this continuous presence,  
5 major demographic changes occurred in wolf populations between the late Pleistocene and  
6 early Holocene, and that extant wolves trace their ancestry to a single late Pleistocene  
7 population. Both the geographic origin of this ancestral population and how it became  
8 widespread remain unknown. Here, we used a spatially and temporally explicit modelling  
9 framework to analyse a large dataset of novel modern and ancient mitochondrial wolf  
10 genomes, spanning the last 50,000 years. Our results suggest that contemporary wolf  
11 populations trace their ancestry to an expansion from Beringia at the end of the Last Glacial  
12 Maximum, and that this process was most likely driven by Late Pleistocene ecological  
13 fluctuations that occurred across the Northern Hemisphere. This study provides direct ancient  
14 genetic evidence that long-range migration has played an important role in the population  
15 history of a large carnivore, and provides an insight into how wolves survived the wave of  
16 megafaunal extinctions at the end of the last glaciation. Moreover, because late Pleistocene  
17 grey wolves were the likely source from which all modern dogs trace their origins, the  
18 demographic history described in this study has fundamental implications for understanding  
19 the geographical origin of the dog.

20

21 **KEYWORDS**

22 Wolves, Ancient DNA, Pleistocene, Megafauna, Population Turnover, Population structure,  
23 ABC, Coalescent modelling

24

1 **1 INTRODUCTION**

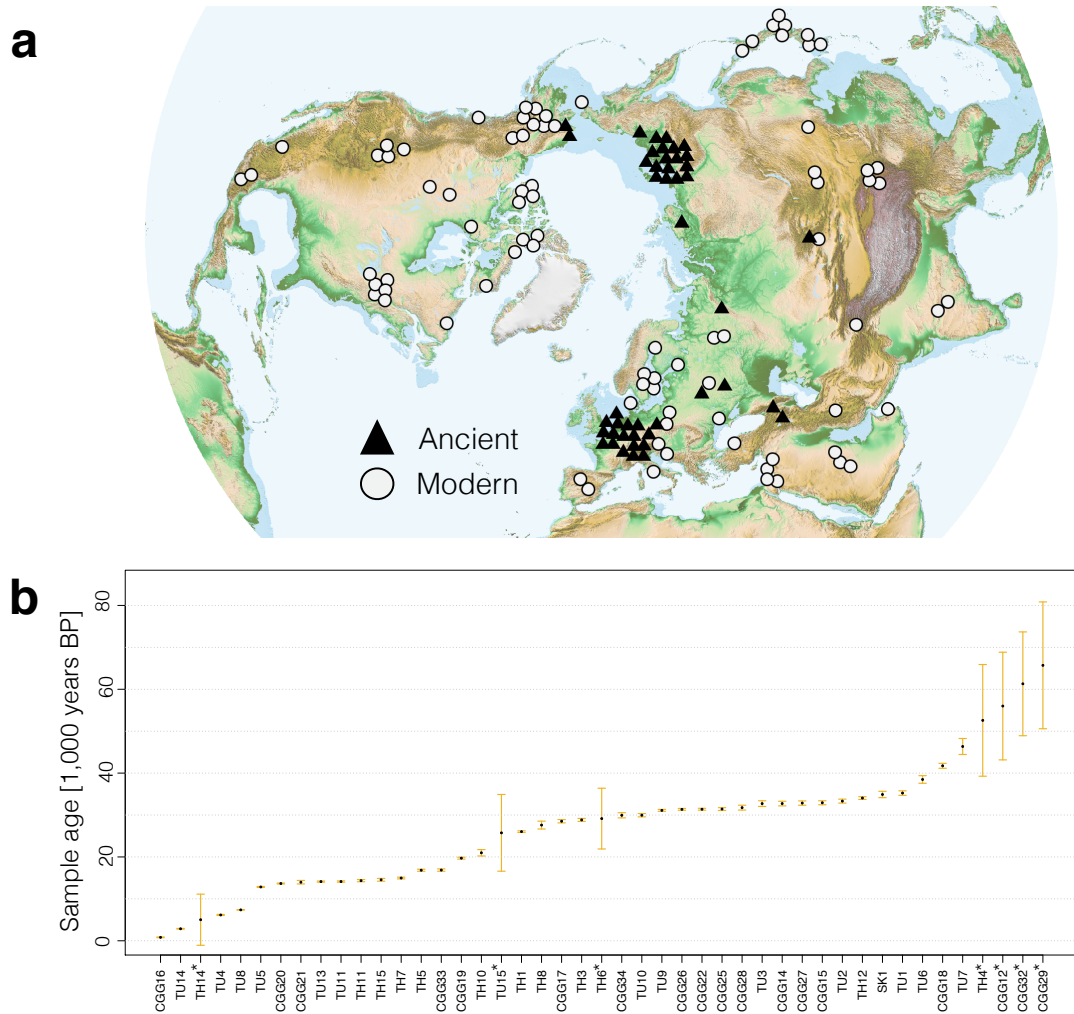
2 The Pleistocene epoch harboured a large diversity of top predators, though most became  
3 extinct during, or soon after the Last Glacial Maximum (LGM), approximately 21,000 years  
4 ago (Barnosky et al. 2004; Clark et al. 2012). The grey wolf (*Canis lupus*) was one of the few  
5 large carnivores that survived and maintained a wide geographical range throughout the  
6 period (Puzachenko and Markova 2016), and both the paleontological and archaeological  
7 records attest to the continuous presence of grey wolves across the Northern Hemisphere for  
8 at least the last 300,000 years (Sotnikova and Rook 2010) (reviewed in Supplementary  
9 Information 1). This geographical and temporal continuity across the Northern Hemisphere  
10 contrasts with analyses of complete modern genomes which have suggested that all  
11 contemporary wolves and dogs descend from a common ancestral population that existed as  
12 recently as 20,000 years ago (Freedman et al. 2014; Skoglund et al. 2015; Fan et al. 2016).

13 These analyses point to a bottleneck followed by a rapid radiation from an ancestral  
14 population around or just after the LGM. The geographic origin and dynamics of this  
15 radiation remain unknown. Resolving these demographic changes is necessary for  
16 understanding the ecological circumstances that allowed wolves to survive the late  
17 Pleistocene megafaunal extinctions. Furthermore, because dogs were domesticated from late  
18 Pleistocene grey wolves (Larson et al. 2012), a detailed insight into wolf demography during  
19 this time period would provide an essential context for reconstructing the history of dog  
20 domestication.

21 Reconstructing past demographic events solely from modern genomes is challenging since  
22 multiple demographic histories can lead to similar genetic patterns in present-day samples  
23 (Groucutt et al. 2015). Analyses that incorporate ancient DNA sequences can eliminate some  
24 of these alternative histories by quantifying changes in population genetic differences through  
25 time. While nuclear markers provide greater power relative to mitochondrial DNA (mtDNA),  
26 the latter is more easily retrievable and better preserved in ancient samples due to its higher  
27 copy number compared to the nuclear DNA, thus allowing for the generation of datasets with  
28 greater geographical and temporal coverage. In particular, analysing samples dated to before,  
29 during and after the demographic events of interest greatly increases the power to infer past  
30 demographic histories. Furthermore, the nuclear mutation rate in canids is poorly understood,  
31 leading to wide date ranges for past demographic events reconstructed from panels of modern  
32 whole genomes (e.g. Freedman et al. 2014; Fan et al. 2016). Having directly dated samples  
33 from a broad time period allows us to estimate mutation rates with higher accuracy and  
34 precision compared to alternative methods (Rambaut 2000; Drummond et al. 2002; Rieux et  
35 al. 2014).

1 Demographic processes, such as range expansions and contractions, that involved space as  
2 well as time are particularly challenging to reconstruct as they often lead to patterns that are  
3 difficult to interpret intuitively (Groucutt et al. 2015). Hypotheses involving spatial processes  
4 can be formally tested using population genetic models that explicitly represent the various  
5 demographic processes and their effect on genetic variation through time and across space  
6 (Eriksson et al. 2012; Eriksson and Manica 2012; Warmuth et al. 2012; Raghavan et al. 2015;  
7 Posth et al. 2016). The formal integration of time and space into population genetics  
8 frameworks allows for the analysis of sparse datasets, a common challenge when dealing with  
9 ancient DNA (Loog et al. 2017).

10 Here, we use a spatially explicit population genetic framework to model a range of different  
11 demographic histories of wolves across the Northern Hemisphere that involve combinations  
12 of population bottlenecks, turnover and long-range migrations as well as local gene flow. To  
13 estimate model parameter and formally test hypotheses of the origin and population dynamics  
14 of the expansion of grey wolves during the LGM, we assembled a substantial dataset (Figure  
15 1, Table S1), spanning the last 50,000 years and the geographic breadth of the Northern  
16 Hemisphere. This dataset consists of 90 modern and 45 ancient wolf whole mitochondrial  
17 genomes (55 of which are newly sequenced). In the following, we first present a  
18 phylogenetic analysis of our sequences and a calibration of the wolf mitochondrial mutation  
19 rates. We then perform formal hypothesis testing using Approximate Bayesian Computation  
20 with our spatio-temporally explicit models. We conclude with a discussion of how our  
21 findings relate to earlier studies and implications for future research.



1  
2 FIGURE 1. Geographic distribution of modern (<500 years old, circles) and ancient (>500  
3 years old, triangles) samples (a) and temporal distribution of ancient samples (b) used in the  
4 analyses. The geographic locations of the samples have been slightly adjusted for clarity (see  
5 Supplementary Table 1 for exact sample locations). \* Samples dated by molecular dating.

6

## 7 2 RESULTS

### 8 2.1 Population Structure of Grey Wolf across the Northern Hemisphere

9 Motivated by the population structure observed in whole genome studies of modern wolves  
10 (Fan et al. 2016), we tested the degree of spatial genetic structure among the modern wolf  
11 samples in our dataset, and found a strong pattern of genetic isolation by distance across  
12 Eurasia ( $\rho=0.3$ ,  $p<0.0001$ ; see Figure S8). Ignoring this population structure (i.e. modelling  
13 wolves as a single panmictic population) can lead to artefactual results (Mazet et al. 2015;  
14 Mazet et al. 2016). The use of spatially structured models, in which migration is restricted to  
15 adjacent populations, is a common approach for dealing with such situations (Kimura and  
16 Weiss 1964; Wegmann et al. 2010; Eriksson et al. 2012; Eriksson and Manica 2012).

1 To capture the observed geographic structure in our dataset, we split the Northern  
2 Hemisphere in seven regions, roughly similar in area (Fig. 3a). The boundaries of these  
3 regions are defined by geographic features, including mountain ranges, seas, and deserts (see  
4 Materials and Methods), which are likely to reduce gene flow (Geffen et al. 2004; Lucchini et  
5 al. 2004) and provide an optimal balance between resolution and power given the distribution  
6 of samples available for analyses. To quantify how well this scheme represents population  
7 structure in modern wolves, we used an AMOVA to separate genetic variance within and  
8 between regions. Our regions capture 24.4% of genetic variation among our modern samples  
9 (AMOVA,  $p < 0.001$ ). This is substantially greater than the approximately 10% of variance  
10 deriving from simple isolation by distance, and supports the hypothesis that the geographic  
11 features (major rivers, deserts and mountain chains) define population structure in  
12 contemporary wolves across the Northern Hemisphere and therefore constitute obstacles to  
13 gene flow (but where the strength of these obstacles may vary).

## 14 **2.2 Bayesian Phylogenetic Analysis**

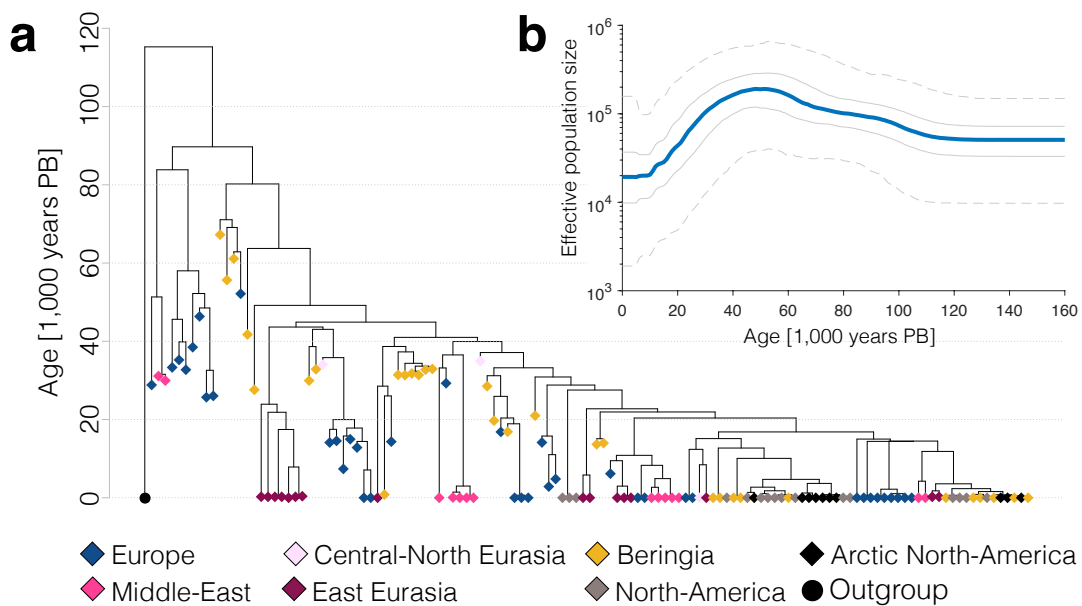
15 All ancient sequences included in the study were subjected to stringent quality criteria with  
16 respect to coverage and damage patterns. Out of the 45 ancient samples 38 had well resolved  
17 direct radiocarbon dates. We joined these ancient sequences with 90 modern mitogenome  
18 sequences and used BEAST (Drummond et al. 2012) to estimate a wolf mitochondrial  
19 mutation rate. By applying the inferred mutation rate we were able to molecularly date the  
20 remaining seven ancient sequences (Materials and Methods). We cross-validated this  
21 approach through a leave-one-out analysis (Materials and Methods) using all the directly  
22 dated ancient sequences and found a very close fit ( $R^2 = 0.86$ ) between the radiocarbon and  
23 the estimated molecular dates and no systematic biases in our molecularly estimated dates  
24 (Figure S9), meriting the inclusion of these sequences and the inferred dates into the spatially  
25 explicit analyses.

26  
27 Our Bayesian phylogenetic analysis suggests that the most recent common ancestor (MRCA)  
28 of all extant North Eurasian and American wolf mitochondrial sequences dates to ca. 40,000  
29 years ago, whereas the MRCA for the combined ancient and modern sequences dates to ca.  
30 90,000 years ago (95% HPD interval: 82,000 – 99,000 years ago) (Figure 2a, see Figs. S11  
31 and S12 for node support values and credibility intervals). A divergent clade at the root of this  
32 tree consists exclusively of ancient samples from Europe and the Middle East that has not  
33 contributed to present day mitochondrial diversity in our data (see also Thalmann et al. 2013).

34 The remainder of the tree consists of a monophyletic clade that is made up of ancient and  
35 modern samples from across the Northern Hemisphere that shows a pattern of rapid

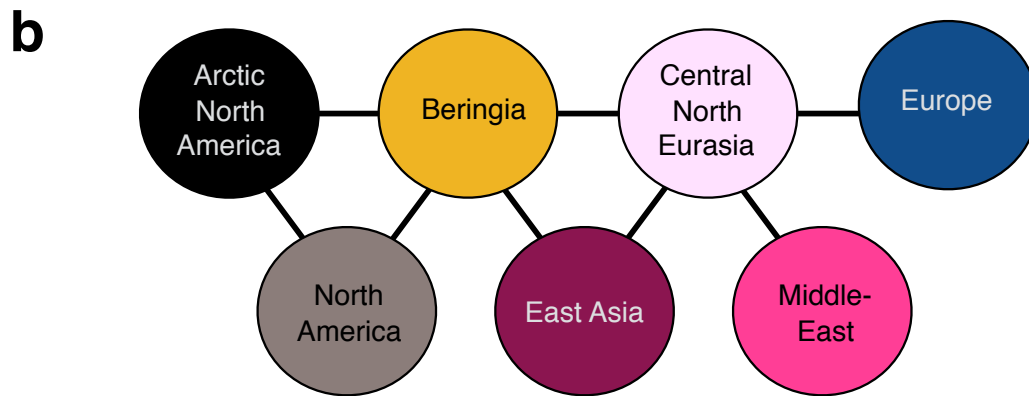
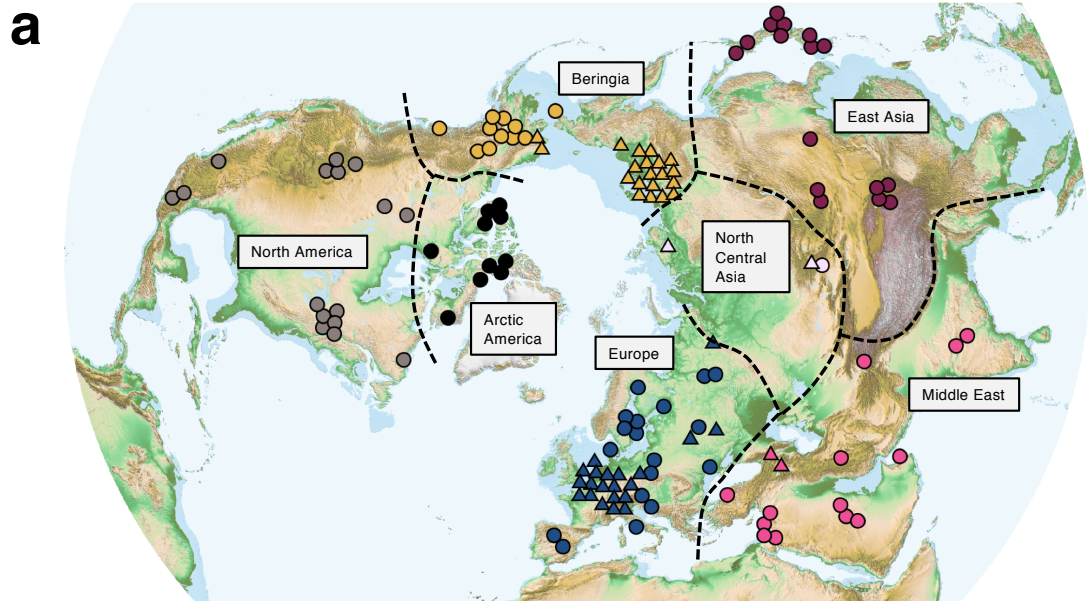
1 bifurcations of genetic lineages centred on 25,000 years ago. To further quantify this temporal  
 2 pattern, we made use of a Bayesian skyline analysis (Figure 2b) that shows a relatively small  
 3 and stable effective genetic population size between ca. 20,000 years ago and the present and  
 4 a decrease in effective population size between ca. 40,000 and 20,000 years ago. This pattern  
 5 is consistent with the scenario suggested in whole genome studies (e.g. Freedman et al. 2014;  
 6 Fan et al. 2016) where wolves had a stable (and likely geographically structured) population  
 7 across the Northern Hemisphere up to a time point between 20,000 and 30,000 years ago,  
 8 when the population experienced a bottleneck that severely reduced genetic variation  
 9 followed by a rapid population expansion.

10 The samples at the root of this clade are predominantly from Beringia, pointing to a possible  
 11 expansion out Northeast Eurasia or the Americas. However, given the uneven temporal and  
 12 geographic distribution of our samples, and the stochasticity of a single genetic marker  
 13 (Nielsen and Beaumont 2009), it is important to explicitly test the extent to which this pattern  
 14 can occur by chance under other plausible demographic scenarios.



15  
 16

17 FIGURE 2. (a) Tip calibrated BEAST tree of all samples used in the spatial analyses  
 18 (diamonds), coloured by geographic region. The circle represents an outgroup (modern Indian  
 19 wolf, not used in the analyses). (b) The effective population size through time from the  
 20 BEAST analysis (Bayesian skyline plot). Solid blue line represents the median estimate and  
 21 the grey lines represent the interquartile range (solid lines) and 95% intervals (dashed lines).



1  
 2 Figure 3: (a) Sample locations and geographic regions, with boundaries indicated by dashed  
 3 lines. The shaded blue line indicates sea levels shallow enough to be land during the last  
 4 glacial maximum (sea depth < 100m). (b) Model network of populations (“demes”),  
 5 connected by gene flow, corresponding to the regions in panel a.

6 **2.3 Spatiotemporal Reconstruction of Past Grey Wolf Demography**

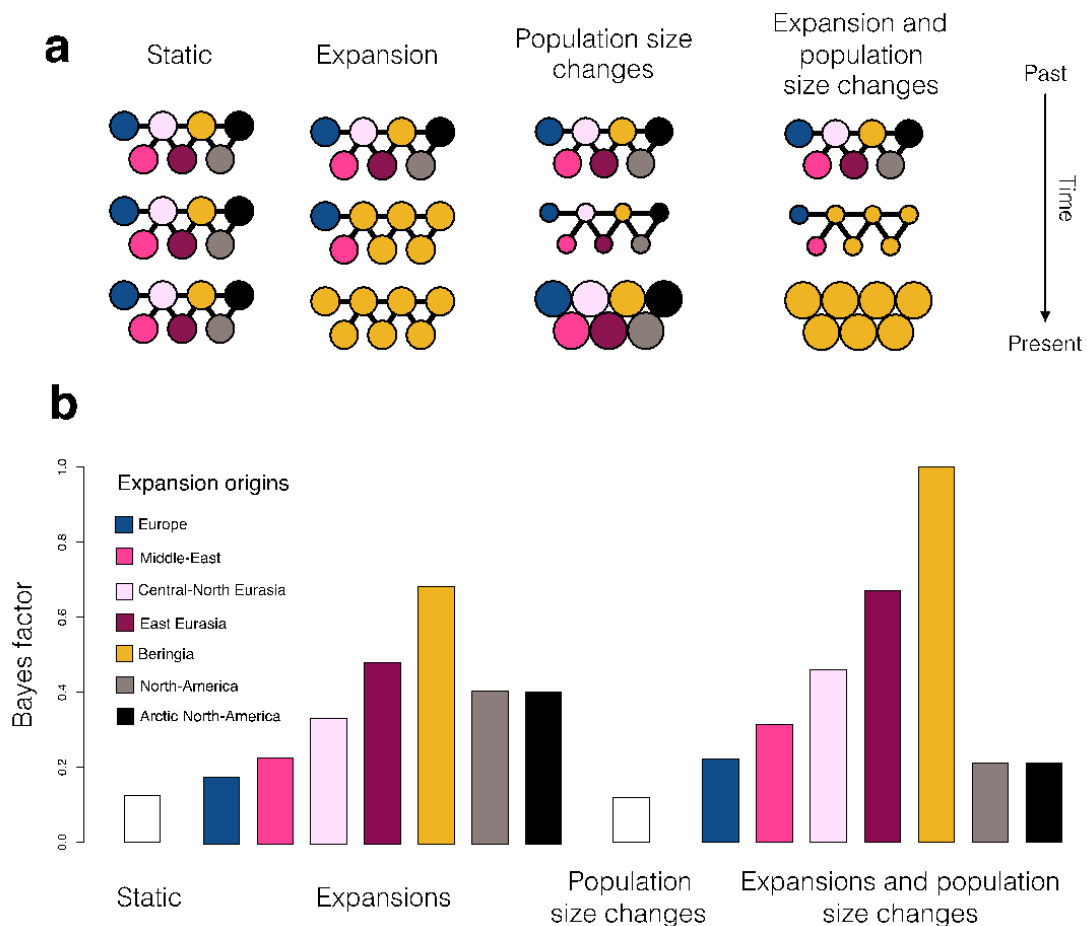
7 Having established the phylogenetic relationship between our samples and population  
 8 structure across the Northern Hemisphere, we tested the ability of different explicit  
 9 demographic scenarios to explain the observed phylogenetic pattern, while also taking into  
 10 account the geographic location and age of each sample. To this end, we represented each of  
 11 the regions in Figure 3a as a population in a network of populations connected by gene flow  
 12 (Figure 3b). We used the coalescent population genetic framework to model genetic evolution  
 13 in this network, in which each deme constitutes a freely mixing and randomly mating  
 14 population. The effective population size of demes, as well as movement of individuals  
 15 between demes, are controlled by parameters covering values that represent different

1 demographic histories.

2 Using this framework we considered a wide range of different explicit demographic scenarios  
3 (illustrated in Figure 3a, see Materials and Methods for details of implementation within the  
4 coalescent framework). The first scenario consisted of a constant population size and uniform  
5 movement between neighbouring demes. This allowed us to test the null hypothesis that drift  
6 within a structured population alone can explain all the patterns observed in the mitochondrial  
7 tree. We then considered two additional demographic processes that could explain the  
8 observed patterns: 1) a temporal sequence of two population size changes that affected all  
9 demes simultaneously (thus allowing for a bottleneck); and 2) an expansion out of one of the  
10 seven demes. In the expansion scenarios, the deme of origin had a continuous population  
11 through time and while in the remaining demes the indigenous populations was sequentially  
12 replaced by the expanding population. Scenario 2 was repeated for all seven possible  
13 expansion origins, thus allowing us to test continuity as well as replacement hypotheses  
14 within each of the seven demes. We considered each demographic event in isolation as well  
15 as their combined effect (resulting in a total of 16 scenarios) and used Approximate Bayesian  
16 Computation (ABC) to calculate the likelihood of each scenario and estimate parameter  
17 values (see Materials and Methods for details).

18 Both the null scenario and the scenario of only population size change in all demes were  
19 strongly rejected (Bayes Factor (BF)  $\leq 0.1$ , Figure 4b and Table S6), illustrating the power of  
20 combining a large dataset of ancient samples with statistical modelling. Scenarios that  
21 combined an expansion and replacement with a change in population size (bottleneck) were  
22 better supported than the corresponding scenarios (i.e. with the same expansion origin) with  
23 constant population size (Figure 4b).

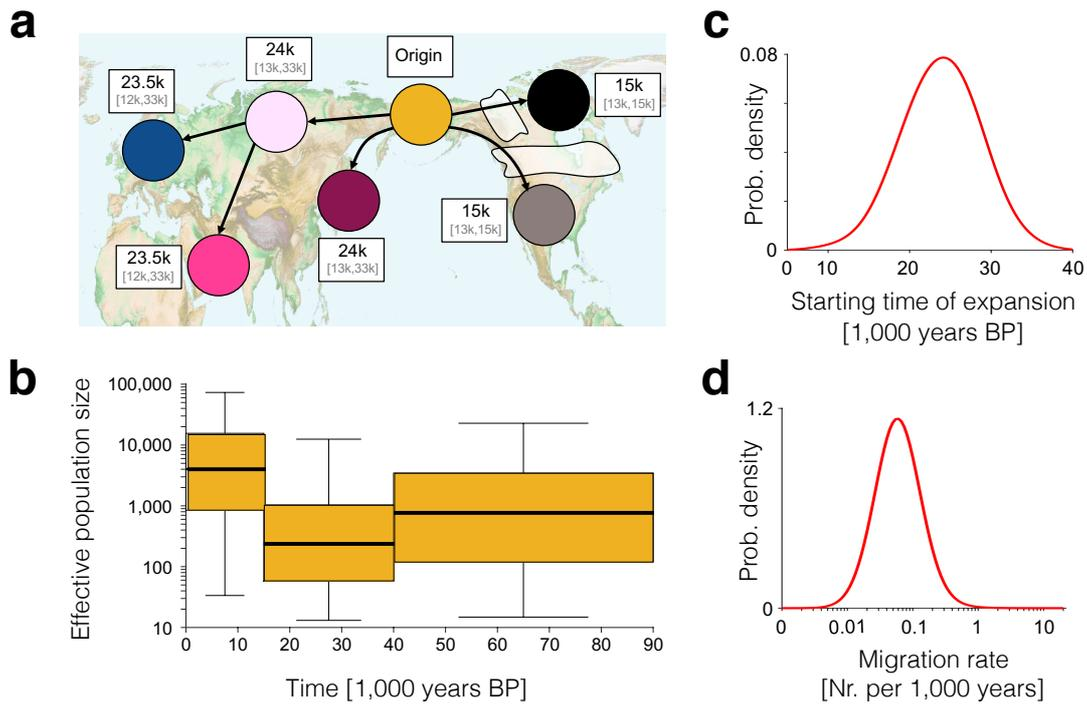
24 The best-supported scenario (Figure 5) was characterized by the combination of a rapid  
25 expansion of wolves out of the Beringian deme approximately 25,000 years ago (95% CI:  
26 33,000-14,000 years ago) with a population bottleneck between 15,000 and 40,000 years ago,  
27 and limited gene flow between neighbouring demes (see Table S7 and Figure S13 for  
28 posterior distributions of all model parameters). We also found relatively strong support for a  
29 scenario that describes a wolf expansion out of the East Eurasian deme (BF 0.7) with nearly  
30 identical parameters to the best-supported scenario (Table S8 & Figure S14). This can be  
31 explained by geographic proximity of East Eurasian and Beringian demes and the genetic  
32 similarity of wolves from these areas.



1  
2

3 FIGURE 4. Spatially and temporally explicit analysis. (a) Illustration of the different  
 4 scenarios, with circles representing one deme each for the seven different geographic regions  
 5 (see panel b for colour legend and text for full description of the scenarios). Solid lines  
 6 represent population connectivity. The *static* scenario (far left) shows stable populations  
 7 through time. The *expansion* scenarios (middle left) shows how one deme (here yellow)  
 8 expands and sequentially replaces the populations in all other demes (from top to bottom).  
 9 The *population size change scenario* (middle right) illustrates how population size in the  
 10 demes can change through time (large or small population size shown as large or small  
 11 circles, respectively). We also show a combined scenario (far right) of both expansion and  
 12 population size change. (b) Likelihood of each demographic scenario relative to the most  
 13 likely scenario, shown as Bayes factors, estimated using Approximate Bayesian Computation  
 14 analyses (see text for details). For expansion scenarios (including the combined expansion  
 15 and population size changes), we colour code each bar according to the origin of the  
 16 expansion (see colour legend).

1



2

3 FIGURE 5. The inferred scenario of wolf demography from the Bayesian analysis using our  
4 spatially and temporally explicit model (see Figure 4 and the main text). (a) Geographic  
5 representation of the expansion scenario (out of Beringia) with median and 95% CI for the  
6 date of the population replacement in each deme given in white boxes next to each deme. (b)  
7 Effective population size (thick line, boxes and whiskers show the median, interquartile range  
8 and 95% CI, respectively, for each time period). (c) Posterior distribution of migration rate  
9 and (d) starting time of expansion.

10

### 11 3 DISCUSSION

#### 12 *Geographic origin of the ancestral wolf population*

13 Recent whole-genome studies (Freedman et al. 2014; Skoglund et al. 2015; Fan et al. 2016)  
14 found that modern grey wolves (*Canis lupus*) across Eurasia are descended from a single  
15 source population. The results of our analyses combining both ancient and modern grey wolf  
16 samples (Figure 1) with a spatially and temporally explicit modelling framework (Figure 4),  
17 suggest that this process began approximately 25,000 (95% CI:33,000-14,000) years ago  
18 when a population of wolves from Beringia (or a Northeast Asian region in close geographic  
19 proximity) expanded outwards and replaced indigenous Pleistocene wolf populations across  
20 Eurasia (Figure 5). This scenario also provides a mechanism explaining the star-like like  
21 topology of modern wolves observed in the whole genome studies (Freedman et al. 2014;  
22 Skoglund et al. 2015; Fan et al. 2016): the expansion was split up by geographic barriers that

1 restricted subsequent gene flow between different branches of the expanding population  
2 which in turn led to the divergence between different sub-populations observed in  
3 contemporary Grey wolves.

4 In the Americas, the Beringian expansion was delayed due to the presence of ice sheets  
5 extending from Greenland to the northern Pacific Ocean (Figure 5) (Raghavan et al. 2015). A  
6 study by Koblmüller et al. (2016) suggested that wolf populations that were extant south of  
7 these ice sheets were replaced by Eurasian wolves crossing the Beringian land bridge. Our  
8 data and analyses support the replacement of North American wolves (following the retreat of  
9 the ice sheets around 16,000 years ago), and our more extensive ancient DNA sampling,  
10 combined with spatially explicit modelling, has allowed us to narrow down the geographic  
11 origin of this expansion to an area between the Lena River in Russia and the Mackenzie River  
12 in Canada also known as Beringia (Hopkins et al. 1982). However, due to lack of Pleistocene  
13 wolf samples that pre-date the retreat of the ice sheets in the area, we are currently not able to  
14 resolve the detailed history of North American wolves. For example, we cannot reject an  
15 alternative scenario where contemporary North American wolves are descendants of a  
16 Pleistocene wolf population that was genetically highly similar to the Beringian population  
17 but existed south of the ice sheets.

18 Thus, despite a continuous fossil record through the late Pleistocene, wolves experienced a  
19 complex demographic history involving population bottlenecks and replacements (Figure 5).  
20 Our analysis suggests that long-range migration played an important role in the survival of  
21 wolves through the wave of megafaunal extinctions at the end of the last glaciation. These  
22 results will enable future studies to examine specific local climatic and ecological factors that  
23 enabled the Beringian wolf population to survive and expand across the Northern  
24 Hemisphere. Furthermore, as the reconstructions in this study are based solely on a maternally  
25 inherited genetic marker, our model was thus only able to address a set of simplified  
26 demographic scenarios (continuity everywhere, or continuity in one location followed by a  
27 replacement expansion from it). Once whole-genome data becomes available, it will likely be  
28 possible to detect contributions from potential refugia at the local scale.

### 29 *Implications for the evolution of grey wolf morphology*

30 Morphological analyses of wolf specimens have noted differences between Late-Pleistocene  
31 and Holocene wolves: late Pleistocene specimens have been described as cranio-dentally  
32 more robust than the present-day grey wolves, as well as having specialized adaptations for  
33 carcass and bone processing (Kuzmina and Sablin 1993; Leonard et al. 2007; Baryshnikov et  
34 al. 2009) associated with megafaunal hunting and scavenging (Fox-Dobbs et al. 2008;  
35 Germonpré et al. 2017). Early Holocene archaeological record has only yielded a single

1 sample with the Pleistocene wolf morphotype (in Alaska) (Leonard et al. 2007), suggesting  
2 that this robust ecomorph had largely disappeared from the Northern Hemisphere by the  
3 Pleistocene-Holocene transition. This change in wolf morphology coincides with a shift in  
4 wolf isotope composition (Bocherens 2015), and the disappearance of megafaunal herbivores  
5 and other large predators such as cave hyenas and cave lions, suggesting a possible change in  
6 the ecological niche of wolves.

7 To date, it has been unclear whether the morphological change was the result of population  
8 replacement (genetic turnover), a plastic response to a dietary shift, or both. Our results  
9 suggest that the Pleistocene-Holocene transition was accompanied by a genetic turnover in  
10 most of the Northern Hemisphere wolf populations as most indigenous wolf populations  
11 experienced a large-scale replacement resulting in the loss of all native Pleistocene genetic  
12 lineages (Figure 5). Similar population dynamics of discontinuity and replacement by  
13 conspecifics have been observed in several other large Pleistocene mammals in Europe  
14 including cave bears, woolly mammoths (Stuart et al. 2004; Palkopoulou et al. 2013), giant  
15 deer (Stuart et al. 2004) and even humans ((Fu et al. 2016; Posth et al. 2016).

16 The geographic exception to this pattern of widespread replacement is Beringia, where we  
17 infer demographic continuity between late Pleistocene and Holocene wolf populations (Figure  
18 5). This finding is at odds with a previous suggestion of genetic turnover in Beringia (Leonard  
19 et al. 2007), probably as the result of differences in both the amount of data available and the  
20 analytical methodology used. Leonard et al. (2007) used a short (427 bases long) segment of  
21 the mitochondrial control region and employed a descriptive phylogeographic approach,  
22 whereas our conclusions are based on an expanded dataset both in terms of sequence length,  
23 sample number, and geographic and temporal range (Figure 1) and formal hypothesis testing  
24 within a Bayesian framework (Figs. 4 and 5).

25 As a consequence, the morphological and dietary shift observed in Beringian wolves between  
26 the late Pleistocene and Holocene (Leonard et al. 2007) cannot be explained by a population  
27 turnover, but instead requires an alternative explanation such as adaptation or plastic  
28 responses to the substantial environmental and ecological changes that took place during this  
29 period. Indeed, grey wolves are a highly adaptable species. Studies of modern grey wolves  
30 have found that differences in habitat - specifically precipitation, temperature, vegetation, and  
31 prey specialization, can strongly affect their cranio-dental morphology (Geffen et al. 2004;  
32 Pilot et al. 2006; O'Keefe et al. 2013; Flower and Schreve 2014; Leonard 2015).

33 The specific causal factors for the replacement of indigenous Eurasian wolves during the  
34 LGM by their Beringian conspecifics (and American wolves following the disappearance of  
35 the Cordilleran and Laurentide ice sheets) are beyond the scope of this study. However, one

1 possible explanation may be related to the relatively stable climate of Beringia compared to  
2 the substantial climatic fluctuations that impacted the rest of Eurasia and Northern America  
3 during the late Pleistocene (Clark et al. 2012). These fluctuations have been associated with  
4 dramatic changes in food webs, leading to the loss of most of the large Pleistocene predators  
5 in the region (Lister and Stuart 2008; Hofreiter and Stewart 2009; Lorenzen et al. 2011;  
6 Bocherens 2015). In addition, the hunting of large Pleistocene predators by Upper  
7 Palaeolithic people (e.g. Münzel and Conard 2004; Germonpré and Hämäläinen 2007; Cueto  
8 et al. 2016) may have also negatively impacted large carnivore populations (Fan et al. 2016).  
9 An interdisciplinary approach involving morphological, isotopic as well as genetic data is  
10 necessary to better understand the relationship between wolf population dynamics and dietary  
11 adaptations in the late Pleistocene and early Holocene period.

#### 12 *Implications for the study of wolf domestication*

13 Lastly, the complex demographic history of Eurasian grey wolves reported here (Figure 5)  
14 also has significant implications for identifying the geographic origin(s) of wolf  
15 domestication and the subsequent spread of dogs. For example, the limited understanding of  
16 the underlying wolf population structure may explain why previous studies have produced  
17 conflicting geographic and temporal scenarios. Numerous previous studies have focused on  
18 the patterns of genetic variation in modern domestic dogs, but have failed to consider  
19 potential genetic variation present in late Pleistocene wolf population, thereby implicitly  
20 assuming a homogeneous wolf population source. As a result, both the domestication and the  
21 subsequent human-mediated movements of dogs were the only processes considered to have  
22 affected the observed genetic patterns in dog populations. However, both domestication from  
23 and admixture with a structured wolf population will have consequences for patterns of  
24 genetic variation within dogs. In light of the complex demographic history of wolves (and the  
25 resulting population genetic structure) reconstructed by our analysis, several of the  
26 geographic patterns of haplotype distribution observed in previous studies, including  
27 differences in levels of diversity found within local dog populations (Wang et al. 2016), and  
28 the deep phylogenetic split between Eastern and Western Eurasian dogs (Frantz et al. 2016),  
29 could have resulted from known admixture between domestic dogs and grey wolves (Verardi  
30 et al. 2006; Godinho et al. 2011; Freedman et al. 2014; Fan et al. 2016). Future analyses  
31 should therefore explicitly include the demographic history of wolves and demonstrate that  
32 the patterns of variation observed within dogs fall outside expectations that take admixture  
33 with geographically structured wolf populations into account.

34

## 35 **4 MATERIALS AND METHODS**

### 36 **4.1 Data preparation**

1 We sequenced whole mitochondrial genomes of 40 ancient and 22 modern wolf samples.  
2 Sample information, including geographic locations, estimated ages and archaeological  
3 context information for the ancient samples, is provided in the Table S1 and Supplementary  
4 Information (SI) 1.2. Of the 40 ancient samples, 24 were directly radiocarbon dated for this  
5 study and calibrated using the IntCal13 calibration curve (see Table S1 for radiocarbon dates,  
6 calibrated age ranges and AMS laboratory reference numbers). DNA extraction, sequencing  
7 and quality filtering, and mapping protocols used are described in SI 2.

8 We included 16 previously published ancient mitochondrial wolf genomes (Table S1 and SI  
9 2). In order to achieve a uniform dataset, we re-processed the raw reads from previously  
10 published samples using the same bioinformatics pipeline as for the newly generated  
11 sequences.

12 We subjected the aligned ancient sequences to strict quality criteria in terms of damage  
13 patterns and missing data (Figs. S3 – S5). First, we excluded all whole mitochondrial  
14 sequences that had more than 1/3 of the whole mitochondrial genome missing (excluding the  
15 mitochondrial control region – see below) at minimum three-fold coverage. Secondly, we  
16 excluded all ancient whole mitochondrial sequences that contained more than 0.1% of  
17 singletons showing signs of deamination damage typical for ancient DNA (C to T or A to G  
18 singletons). After quality filtering, we were left with 32 newly sequenced and 13 published  
19 ancient whole mitochondrial sequences (Table S1).

20 We also excluded sequences from archaeological specimens that postdate the end of  
21 Pleistocene and that have been identified as dogs (Table S1), since any significant population  
22 structure resulting from a lack of gene flow between dogs and wolves could violate the  
23 assumption of a single, randomly mating canid population. Some of the Pleistocene  
24 specimens used in the demographic analyses (TH5, TH12, TH14) have been argued to show  
25 features commonly found in modern dogs and have therefore been suggested to represent  
26 Paleolithic dogs (e.g. Sablin and Khlopachev 2002; Germonpré et al. 2009; Germonpré et al.  
27 2012; Druzhkova et al. 2013; Germonpré et al. 2015). Here, we disregard such status calls  
28 because of the controversy that surrounds them (Crockford and Kuzmin 2012; Morey 2014;  
29 Drake et al. 2015; Perri 2016), and because early dogs would have been genetically similar to  
30 the local wolf populations from which they derived. This reasoning is supported by the close  
31 proximity of these samples to other wolf specimens confidently described as wolves in the  
32 phylogenetic tree (see Figure S10).

33 Finally, we added 66 modern published wolf sequences from NCBI and two sequences from  
34 (Freedman et al. 2014) (Table S1) resulting in a final dataset of 135 complete wolf

1 mitochondrial genome sequences, of which 45 were ancient and 90 were modern. We used  
2 ClustalW alignment tool (version 2.1) (Larkin et al. 2007) to generate a joint alignment of all  
3 genomes. In order to avoid the potentially confounding effect of recurrent mutations in the  
4 mitochondrial control region (Excoffier and Yang 1999) in pairwise difference calculations,  
5 we removed this region from all subsequent analyses. This resulted in an alignment of  
6 sequences 15,466 bp in length, of which 1301 sites (8.4%) were variable. The aligned dataset  
7 is located in Supplementary File S1.

#### 8 **4.2 Phylogenetic analysis**

9 We calculated the number of pairwise differences between all samples (Figure S6) and  
10 generated a neighbour-joining tree based on pairwise differences (Figure S7). This tree shows  
11 a clade consisting of samples exclusively from the Tibetan region and the Indian sub-  
12 continent that are deeply diverged from all ancient and other modern wolf samples (see also  
13 Sharma et al. 2004; Aggarwal et al. 2007). A recent study of whole genome data showed a  
14 complex history of South Eurasian wolves (Fan et al. 2016) that is beyond the scope of our  
15 study. While their neighbour-joining phylogeny grouped South Eurasian wolves with East  
16 and North East Asian wolves (Figure 3 in (Fan et al. 2016), they cluster outside of all other  
17 grey wolves in a Principal Component Analysis (Figure 4 in (Fan et al. 2016), and also show  
18 a separate demographic history within a PSMC analysis (Figure 5 in (Fan et al. 2016).  
19 Because our study did not possess sufficient samples from the Himalayas and the Indian  
20 subcontinent to unravel their complex demography, we excluded samples from these regions  
21 and focused on the history of North Eurasian and North American wolves, for which we have  
22 good coverage through time and space.

23 We used PartitionFinder (Lanfear et al. 2012) and BEAST (v.1.8.0) (Drummond et al. 2012)  
24 to build a tip calibrated wolf mitochondrial tree (with a strict global clock, see SI 3.2 for full  
25 details) from modern and directly dated ancient samples, and to estimate mutation rates for  
26 four different partitions of the wolf mitochondrial genome (see Tables S3 and S4 for results).

27 We used BEAST to molecularly date seven sequences from samples that were not directly  
28 radiocarbon dated (TH4, TH6, TH14, TU15) or that had been dated to a period beyond the  
29 limit of reliable radiocarbon dating (>48,000 years ago) (CGG12, CGG29, CGG32). We  
30 estimated the ages of the samples by performing a BEAST run where the mutation rate was  
31 fixed to the mean estimates from the previous BEAST analysis and all other parameter  
32 settings were set as described in the SI 3.2. We cross-validated this approach through a leave-  
33 one-out analysis where we sequentially removed a directly dated sample and estimated its  
34 date as described above. We find a close fit ( $R^2=0.86$ ) between radiocarbon and molecular  
35 dates (Figure S9). We combined the seven undated samples with the 110 ancient and modern

1 samples from the previous run and used a uniform prior ranging from 0 to 100,000 years to  
2 estimate the ages of the seven undated samples (see Table S5 for results).

3 Finally, in order to estimate the mitochondrial divergence time between the South Eurasian  
4 (Tibetan and Indian) and the rest of our wolf samples, we performed an additional BEAST  
5 run in which we included all modern and ancient grey wolves ( $N = 129$ ) as well as five  
6 Tibetan and one Indian wolf, and used parameters identical to the ones described above. The  
7 age of the ancient samples was set as the mean of the calibrated radiocarbon date distribution  
8 (for radiocarbon dated samples) or as the mean of the age distribution from the BEAST  
9 analyses (for molecularly dated samples).

#### 10 **4.3 Isolation by distance analysis**

11 We performed isolation by distance (IBD) analyses to see the extent to which wolf  
12 mitochondrial genetic variation shows population structure. To this end, we regressed the  
13 pairwise geographic distances between 84 modern wolf samples (Table S1) against their  
14 pairwise genetic (mitochondrial) distances. The geographic distance between all sample pairs  
15 was calculated in kilometres as the great circle distance from geographic coordinates, using  
16 the Haversine Formula (Sinnott 1984) to account for the curvature of the Earth as follows:

$$17 \quad G_{ij} = 2r \arcsin \left( \sqrt{\sin^2((\varphi_j - \varphi_i)/2)^2 + \cos(\varphi_i) \cos(\varphi_j) \sin^2((\lambda_i - \lambda_j)/2)^2} \right) [1]$$

18 Where  $G$  is the distance in kilometres between individuals  $i$  and  $j$ ;  $\varphi_i$  and  $\varphi_j$  are the latitude  
19 coordinates of individuals  $i$  and  $j$ , respectively;  $\lambda_i$  and  $\lambda_j$  are the longitude coordinates of  
20 individuals  $i$  and  $j$ , respectively; and  $r$  is the radius of the earth in kilometres. The pairwise  
21 genetic distances were calculated as the proportion of sites that differ between each pair of  
22 sequences (excluding the missing bases), using *dist.dna* function in the R package APE  
23 (Paradis et al. 2004).

#### 24 **4.4 Geographical deme definitions**

25 We represented the wolf geographic range as seven demes, defined by major geographic  
26 barriers through time.

- 27 1. The *European* deme is bordered by open water from the North and the West (the  
28 Arctic and the Atlantic oceans, respectively); the Ural Mountains from the East; and  
29 the Mediterranean, the Black and the Caspian Sea and the Caucasus mountains from  
30 the South.
- 31 2. The *Middle-Eastern* deme consists of the Arabian Peninsula, Anatolia and  
32 Mesopotamia and is bordered by the Black Sea, the Caspian Sea and the Aral Sea in

1 the North; the Indian Ocean in the South; the Tien Shen mountain range, the Tibetan  
2 Plateau and the Himalayas from the East; and the Mediterranean Sea in the West.

3 3. The *Central North Eurasian* deme consist of the Siberian Plateau and is bordered by  
4 the Arctic Ocean from the North; the Ural Mountains from the West; the Lena River  
5 and mountain ranges of North Eastern Siberia (Chersky and Verkhoyansk ranges)  
6 from the East; and the Tien Shen mountain range, the Tibetan Plateau and the Gobi  
7 Desert from South-East.

8 4. The *East Eurasian deme* is bordered by the Tien Shen mountain range, the Tibetan  
9 Plateau and Gobi desert from the West; the Pacific Ocean from the East; and the Lena  
10 river and the mountain ranges of North Eastern Siberia (Chersky and Verkhoyansk  
11 ranges) from the North.

12 5. The *Beringia* deme spans the Bering Strait, which was a land bridge during large  
13 parts of the Late Pleistocene and the Early Holocene. It is bordered to the West by the  
14 Lena River and mountain ranges of North Eastern Siberia (Chersky and Verkhoyansk  
15 ranges), and to the South and East by the extent of the Cordillerian and Laurentide ice  
16 sheets during the Last Glacial Maximum.

17 6. The *Arctic North America* deme consists of an area of the North American continent  
18 east of the Rocky Mountains and west of Greenland, that was covered by ice during  
19 the last Glaciation and is at present known as the Canadian Arctic Archipelago.

20 7. The *North America* deme consists of an area in the Northern American sub-continent  
21 up to and including the area that was covered by the Cordillerian and Laurentide ice  
22 sheets during the last glaciation (Raghavan et al., 2015).

23

#### 24 **4.5 Amova analyses**

25 To quantify the extent our geographic demes capture genetic variation in the data we  
26 performed an AMOVA analyses (Excoffier et al. 1992) We calculated the pairwise genetic  
27 distance between all modern wolf ( $n = 84$ , Table S1) sample pairs as described above (Section  
28 4.3, Isolation by distance analysis) and partitioned the samples, based on their geographic  
29 locations, into 7 populations corresponding the geographical demes, described in Section 4.4,  
30 Geographical deme definitions. We used these demes as the level of analyses and performed 1  
31 million permutations using the *amova* function in the *R* package *pegas* (v 0.10). We found  
32 strong support for our geographical demes ( $p < 10^{-6}$ ) with 24.4% of the variance within the  
33 dataset explained by the chosen demes.

34

#### 35 **4.6 Demographic scenarios**

1 We tested a total of 16 demographic scenario combinations, from four different kinds of  
2 demographic scenarios (illustrated in Figure 4a in the main text):

3 1) Static model (the null hypothesis) – neighbouring demes exchange migrants, no  
4 demographic changes.

5 2) Bottleneck scenarios – demes exchange migrants as in the static model but  
6 populations have different size in different time periods. We consider three time  
7 periods: 0-15,000 years ago, 15,000-40,000 years ago, and >40,000 years ago.

8 3) Expansion scenarios - demes exchange migrants like in the static model but a single  
9 deme (which itself has a continuous population through time) experiences an  
10 expansion starting between 5,000 and 40,000 years ago (at a minimum rate of 1,000  
11 years per deme, so the whole world could be colonized within 3,000 years or faster).  
12 The deme of origin has a continuous population through time while native  
13 populations in all other demes experience replacement – allowing us to formally test  
14 both the continuity and replacement hypotheses in each of the demes.

15 4) Combinations of scenarios 2 & 3.

#### 16 **4.7 Population genetic coalescent framework**

17 We implemented coalescent population genetic models for the different demographic  
18 scenarios to sample gene genealogies.

19 In the static scenario, we simulated local coalescent processes (Kingman 1982) within each  
20 deme (scaled to rate  $1/K$  per pair of lineages, where  $K$  is the mean time to most recent  
21 common ancestor in a deme and is thus proportional to the effective population size). In  
22 addition, we moved lineages between demes according to a Poisson process with rate  $m$  per  
23 lineage. To match the geographic and temporal distribution of the data, we represented each  
24 sample with a lineage from the corresponding deme and date.

25 The bottleneck scenario was implemented as the static one but with piecewise constant values  
26 for  $K$  as a function of time. We considered three time periods, each with its own value of  $K$   
27 ( $K_1$ ,  $K_2$  and  $K_3$ ), motivated by the archaeological and genetic evidence of wolf population  
28 changes described in the main text. The first time period was from present to early Holocene,  
29 0-15,000 years ago. The second time period extended from early Holocene to late Pleistocene  
30 and covered the last glacial maximum, 15,000-40,000 years ago. Finally, the third time period  
31 covered the late Pleistocene and beyond, i.e. 40,000 years ago and older.

32 The population expansion scenarios were based on the static model but with an added  
33 population expansion model with founder effects and replacement of local populations (we  
34 refer to populations not yet replaced by the expansion as "indigenous"). Starting at time  $T$ , the

1 population expanded from the initial deme and replaced its neighbouring populations. The  
2 population at the deme of origin was represented as a continuous population through time.  
3 After the start of the expansion, the expansion proceeded in fixed steps of  $\Delta T$  (in time). At  
4 each step, colonized populations replaced neighbouring indigenous populations (if an  
5 indigenous deme bordered to more than one colonized deme, these demes contributed equally  
6 to the colonization of the indigenous deme). In the coalescent framework (that simulates gene  
7 genealogies backwards in time) the colonization events corresponds to forced migrations from  
8 the indigenous deme to the source deme. If there were more than one source deme, the source  
9 of each lineage was chosen randomly with equal probability. Finally, founder effects during  
10 the colonization of an indigenous deme were implemented as a local, instantaneous  
11 population bottleneck in the deme (after the expansion), with a severity scaled to give a fixed  
12 probability  $x$  of a coalescent event for each pair of lineages in the deme during the bottleneck  
13 (Eriksson and Mehlig 2004). ( $x=1$  correspond to a complete loss of genetic diversity in the  
14 bottleneck, and  $x=0$  corresponds to no reduction in genetic diversity.)

15 Finally, the combined scenario of population expansion and bottlenecks was implemented by  
16 making the population size parameter  $K$  in the population expansion model time dependent as  
17 in the population bottleneck model.

#### 18 **4.8 Approximate Bayesian Computation analysis**

19 We used Approximate Bayesian Computation (ABC) analysis (Beaumont et al. 2002) with  
20 ABCtoolbox (Wegmann et al. 2010) to formally test the fit of our different demographic  
21 models. This approach allows formal hypothesis testing using likelihood ratios in the cases  
22 where the demographic scenarios are too complex for a direct calculation of the likelihoods  
23 given the models. We used the most likely tree from BEAST (see SI 3.2 for details) as data,  
24 and simulated trees using the coalescent simulations described above.

25 To match the assumption of random mixing within each deme in the population genetic  
26 model, we removed closely related sequences if they came from the same geographic location  
27 and time period, by randomly retaining one of the closely related sequences to be included in  
28 the analysis (Table S1, column “Samples\_used\_in\_Simulation\_Analysis”).

29 To robustly measure differences between simulated and observed trees we use the matrix of  
30 time to most recent common ancestor (TMRCA) for all pairs of samples. This matrix also  
31 captures other allele frequency based quantities frequently used as summary statistics with  
32 ABC, such as  $F_{ST}$ , as they can be calculated from the components of this matrix.

1 In principle the full matrix could be used, but in practice it is necessary to use a small number  
2 of summary statistics for ABC to work properly (Wegmann et al. 2010). To this end, we  
3 computed the mean TMRCA between pairs of sequences either within or between 1) Europe,  
4 2) Middle East, 3) North East Eurasia, Beringia and East Eurasia combined; and 4) Artic and  
5 Continental North America combined. This strategy is based on geographic proximity and  
6 genetic similarity in the dataset. We note that this is not the same as modelling the combined  
7 demes as a single panmictic deme; structure between the demes is still modelled explicitly,  
8 but the summary statistics are averaged over multiple demes.

9 An initial round of fitting the model showed that all scenarios underestimate the deme  
10 TMRCA for the Middle East, while the rest of the summary statistics were well captured by  
11 the best fitting demographic scenarios. This could be explained by a scenario where the  
12 Middle East was less affected by the reduction in population size during the last glacial  
13 maximum. However, we currently lack sufficient number of samples from this area to  
14 explicitly test a more complex scenario such as this hypothesis. To avoid outliers biasing the  
15 likelihood calculations in ABC (Wegmann et al. 2010) we removed this summary statistic,  
16 resulting in nine summary statistics in total.

17 For each of the 16 scenarios we performed 1 billion simulations with randomly chosen  
18 parameter combinations, chosen from the following parameter intervals for the different  
19 scenarios:

- 20 • The static scenario:  $m$  in  $[0.001,20]$  and  $K$  in  $[0.01,100]$ .
- 21 • The bottleneck scenarios:  $m$  in  $[0.001,20]$  and  $K_1, K_2, K_3$  in  $[0.01,100]$ .
- 22 • The expansion scenarios:  $m$  in  $[0.001,20]$ ,  $K$  in  $[0.01,100]$ ,  $x$  in  $[0,1]$ ,  $T$  in  $[5,40]$  and  
23  $\Delta T$  in  $[0.001,1]$ . For expansion out of the North American scenario and the expansion  
24 out of the Arctic North American scenario, the glaciation and during the LGM in  
25 North American and sea level rise during the de-glaciation mean that  $T$  must be in the  
26 range  $[9,16]$
- 27 • The combined bottleneck and expansion scenarios:  $m$  in  $[0.001,20]$ ,  $K_1, K_2, K_3$  in  
28  $[0.01,100]$ ,  $x$  in  $[0,1]$ ,  $T$  in  $[5,40]$  and  $\Delta T$  in  $[0.001,1]$ .

29 The parameter  $m$  is measured in units of 1/1,000 years, and  $T$ ,  $\Delta T$ ,  $K$ ,  $K_1$ ,  $K_2$  and  $K_3$  are  
30 measured in units of 1,000 years. The parameters  $x$ ,  $T$  and  $\Delta T$  were sampled according to a  
31 uniform distribution over the interval, while all other parameters were sampled from a  
32 uniform distribution of their log-transformed values. To identify good parameter  
33 combinations for ABC, we first calculated the Euclidian square distances between predicted  
34 and observed statistics and restricted analysis to parameter combinations within the lowest  
35 tenth distance percentile. We then ran the ABCtoolbox (Wegmann et al. 2010) on the

1 accepted parameter combinations to estimate posterior distributions of the model parameters,  
2 and to calculate the likelihood of each scenario as described in the ABCtoolbox manual.

3 See Table S6 for ABC likelihoods and Bayes factors for all demographic scenarios tested. See  
4 Tables S7 and S8 for posterior probability estimates and Figs. S13 and S14 for posterior  
5 density distributions for estimated parameters ( $\Delta T$ ,  $T$ ,  $\log_{10} K_1$ ,  $\log_{10} K_2$ ,  $\log_{10} K_3$ ,  $\log_{10} m$ ,  $x$ ) in  
6 the two most likely models (An expansion out of Beringia with a population size change and  
7 an expansion out of East Eurasia with a population size change).

#### 8 **4.9. Map plots**

9 The background map used in Figure 1, panel a and Figure 3 panel a, showing climatic regions  
10 on land masses, was generated by downloading the file color\_etopo1\_ice\_low.jpg from  
11 ETOPO1 (Amante and Eakins 2016) , a one arc-minute global relief model of Earth's surface  
12 that integrates land topography and ocean bathymetry, and masking out regions where sea  
13 depths are greater than 100m.

#### 14 **ACKNOWLEDGEMENTS**

15 The authors are grateful to Daniel Klingberg Johansson & Kristian Murphy Gregersen from  
16 the Natural History Museum of Denmark; Gabriella Hürlimann from the Zurich Zoo; Jane  
17 Hopper from the Howlett's & the Port Lympne Wild Animal Parks; Cyrintha Barwise-Joubert  
18 & Paul Vercammen from the Breeding Centre for Endangered Arabian Wildlife; Link Olson  
19 from the University of Alaska Museum of the North; Joseph Cook & Mariel Campbell from  
20 the Museum of Southwestern Biology; Lindsey Carmichael & David Coltman from the  
21 University of Alberta; North American Fur Auctions; Department of Environment Nunavut  
22 and Environment and Natural Resources Northwest Territories for DNA samples from the  
23 modern wolves. The authors are also grateful to the staff at the Danish National High-  
24 Throughput Sequencing Centre for technical assistance in the data generation; the Qimmeq  
25 project, funded by The Velux Foundations and Aage og Johanne Louis-Hansens Fond, for  
26 providing financial support for sequencing ancient Siberian wolf samples; the Rock  
27 Foundation (New York, USA) for supporting radiocarbon dating of ancient samples from the  
28 Yana site; to Stephan Nylander from the Swedish Museum of Natural History for advice on  
29 phylogenetic analyses and Terry Brown from the University of Manchester for comments on  
30 this manuscript. L.L., K.D. & G.L. were supported by Natural Environment Research  
31 Council, UK (grant numbers NE/K005243/1, NE/K003259/1); LL. was also supported by the  
32 European Research Council grant (339941-ADAPT); A.M. & A.E. were supported by the  
33 European Research Council Consolidator grant (grant number 647787-LocalAdaptation); L.F.  
34 & G.L. were supported by the European Research Council grant (ERC-2013-StG 337574-  
35 UNDEAD); T.G was supported by European Research Council Consolidator grant (681396-

1 Extinction Genomics) & Lundbeck Foundation grant (R52-5062); O.T. was supported by the  
2 National Science Center, Poland (2015/19/P/NZ7/03971) with funding from EU's Horizon  
3 2020 program under the Marie Skłodowska-Curie grant agreement (665778) and Synthesys  
4 Project (BETAF 3062); V.P., E.P. & P.N. were supported by the Russian Science Foundation  
5 grant (N16-18-10265 RNF); A.P. was supported by the Max Planck Society; M.L-G. was  
6 supported by Czech Science Foundation grant (GAČR15-06446S).

#### 7 **AUTHOR CONTRIBUTIONS**

8 L.L., O.T., M.T.P.G., J.K., G.L., A.E. and A.M. designed the research; O.T., M-H.S.S.,  
9 V.J.S., K.E.W., M.S.V., I.K.C.L., N.W. and G.S. performed ancient DNA laboratory work  
10 with input from J.K., M.T.P.G., H.S., K-H.H., R.S.M. and K-H.H.; M-H.S.S. performed  
11 modern DNA laboratory work with input from M.T.P.G; O.T., J.A.S.C. and L.L. performed  
12 bioinformatic analyses; L.L., A.E. and A.M. designed the population genetic analyses; L.L.  
13 performed phylogenetic analyses; A.E. implemented the spatial analyses framework; L.L. and  
14 A.E. performed spatial analyses; M.G., J.B., V.V.P., E.Y.P., P.A.N., S.E.F., J.E-L., A.W.K.,  
15 B.G., H.N., H-P.U. and M.L-G. provided samples; V.V.P., M.G., M. L-G., H.B., H.N.,  
16 A.W.K., E.Y.P. and P.A.N. provided context for archaeological samples; A.P., M.G., H.B.  
17 and K.D. helped setting the results of genetic analyses into an archaeological context; A.M.,  
18 M.T.P.G., A.J.H., G.L., J.K., E.W. and K.D. secured funding for the project; L.L., O.T. and  
19 A.E. wrote the initial draft of the manuscript with input from A.M.; L.L., O.T. and A.E. wrote  
20 the manuscript and the supplementary information with input from A.P., M.G., H.B., M-  
21 H.S.S., M.T.P.G., K.E.W., A.M., G.L. and K.D.; V.J.S., L.F., A.W.K., K-H.H., A.J.H.,  
22 R.S.M., H.S., G.S., V.V.P., E.Y.P., P.A.N. and J.E-L. provided comments to the manuscript  
23 and/or to the supplementary information.

#### 24 **DATA AVAILABILITY**

25

26 The assembled mitochondrial genomes are available from GenBank (accession numbers  
27 MK936995-MK937053 (ancient) and MN071185-MN071206 (modern)). The raw sequencing  
28 reads used for generating novel ancient mitochondrial genomes can be retrieved from the  
29 European Nucleotide Archive under the study number: PRJEB32023.” The code for  
30 population genetic simulations of all tested scenarios and scripts for preliminary and output  
31 analyses are available on GitHub repository <https://github.com/LiisaLoog/pleistocene-wolves>.

32

1 **REFERENCES**

- 2 Aggarwal RK, Kivisild T, Ramadevi J, Singh L. 2007. Mitochondrial DNA coding region  
3 sequences support the phylogenetic distinction of two Indian wolf species. *Journal*  
4 *of Zoological Systematics and Evolutionary Research* 45:163–172.
- 5 Amante C, Eakins BW. 2016. ETOPO1 1 Arc-Minute Global Relief Model: Procedures, Data  
6 Sources and Analysis. NOAA Technical Memorandum NESDIS NGDC-24. Available  
7 from: <https://www.ngdc.noaa.gov/mgg/global/>
- 8 Barnosky AD, Koch PL, Feranec RS, Wing SL, Shabel AB. 2004. Assessing the Causes of Late  
9 Pleistocene Extinctions on the Continents. *Science* 306:70–75.
- 10 Baryshnikov GF, Mol D, Tikhonov AN. 2009. Finding of the Late Pleistocene carnivores in  
11 Taimyr Peninsula (Russia, Siberia) with paleoecological context. *Russian Journal of*  
12 *Theriology* 8:107–113.
- 13 Beaumont MA, Zhang W, Balding DJ. 2002. Approximate Bayesian Computation in  
14 Population Genetics. *Genetics* 162:2025–2035.
- 15 Bocherens H. 2015. Isotopic tracking of large carnivore palaeoecology in the mammoth  
16 steppe. *Quaternary Science Reviews* 117:42–71.
- 17 Clark PU, Shakun JD, Baker PA, Bartlein PJ, Brewer S, Brook E, Carlson AE, Cheng H, Kaufman  
18 DS, Liu Z, et al. 2012. Global climate evolution during the last deglaciation. *PNAS*  
19 109:E1134–E1142.
- 20 Crockford SJ, Kuzmin YV. 2012. Comments on Germonpré et al., *Journal of Archaeological*  
21 *Science* 36, 2009 “Fossil dogs and wolves from Palaeolithic sites in Belgium, the  
22 Ukraine and Russia: osteometry, ancient DNA and stable isotopes”, and Germonpré,  
23 Lázkíčková-Galetová, and Sablin, *Journal of Archaeological Science* 39, 2012  
24 “Palaeolithic dog skulls at the Gravettian Předmostí site, the Czech Republic.”  
25 *Journal of Archaeological Science* 39:2797–2801.
- 26 Cueto M, Camarós E, Castaños P, Ontañón R, Arias P. 2016. Under the Skin of a Lion: Unique  
27 Evidence of Upper Paleolithic Exploitation and Use of Cave Lion (*Panthera spelaea*)  
28 from the Lower Gallery of La Garma (Spain). *PLOS ONE* 11:e0163591.
- 29 Drake AG, Coquerelle M, Colombeau G. 2015. 3D morphometric analysis of fossil canid skulls  
30 contradicts the suggested domestication of dogs during the late Paleolithic.  
31 *Scientific Reports* 5:8299.
- 32 Drummond AJ, Nicholls GK, Rodrigo AG, Solomon W. 2002. Estimating Mutation Parameters,  
33 Population History and Genealogy Simultaneously From Temporally Spaced  
34 Sequence Data. *Genetics* 161:1307–1320.
- 35 Drummond AJ, Suchard MA, Xie D, Rambaut A. 2012. Bayesian Phylogenetics with BEAUti  
36 and the BEAST 1.7. *Mol Biol Evol* 29:1969–1973.
- 37 Druzhkova AS, Thalmann O, Trifonov VA, Leonard JA, Vorobieva NV, Ovodov ND,  
38 Graphodatsky AS, Wayne RK. 2013. Ancient DNA Analysis Affirms the Canid from  
39 Altai as a Primitive Dog. *PLOS ONE* 8:e57754.

- 1 Eriksson A, Betti L, Friend AD, Lycett SJ, Singarayer JS, Cramon-Taubadel N von, Valdes PJ,  
2 Balloux F, Manica A. 2012. Late Pleistocene climate change and the global expansion  
3 of anatomically modern humans. *PNAS* 109:16089–16094.
- 4 Eriksson A, Manica A. 2012. Effect of ancient population structure on the degree of  
5 polymorphism shared between modern human populations and ancient hominins.  
6 *PNAS* 109:13956–13960.
- 7 Eriksson A, Mehlig B. 2004. Gene-history correlation and population structure. *Phys. Biol.*  
8 1:220.
- 9 Excoffier L, Smouse PE, Quattro JM. 1992. Analysis of molecular variance inferred from  
10 metric distances among DNA haplotypes: application to human mitochondrial DNA  
11 restriction data. *Genetics* 131:479–491.
- 12 Excoffier L, Yang Z. 1999. Substitution rate variation among sites in mitochondrial  
13 hypervariable region I of humans and chimpanzees. *Mol Biol Evol* 16:1357–1368.
- 14 Fan Z, Silva P, Gronau I, Wang S, Armero AS, Schweizer RM, Ramirez O, Pollinger J, Galaverni  
15 M, Del-Vecchio DO, et al. 2016. Worldwide patterns of genomic variation and  
16 admixture in gray wolves. *Genome Res.* 26:163–173.
- 17 Flower LOH, Schreve DC. 2014. An investigation of palaeodietary variability in European  
18 Pleistocene canids. *Quaternary Science Reviews* 96:188–203.
- 19 Fox-Dobbs K, Leonard JA, Koch PL. 2008. Pleistocene megafauna from eastern Beringia:  
20 Paleocological and paleoenvironmental interpretations of stable carbon and  
21 nitrogen isotope and radiocarbon records. *Palaeogeography, Palaeoclimatology,*  
22 *Palaeoecology* 261:30–46.
- 23 Frantz LAF, Mullin VE, Pionnier-Capitan M, Lebrasseur O, Ollivier M, Perri A, Linderholm A,  
24 Mattiangeli V, Teasdale MD, Dimopoulos EA, et al. 2016. Genomic and  
25 archaeological evidence suggest a dual origin of domestic dogs. *Science* 352:1228.
- 26 Freedman AH, Gronau I, Schweizer RM, Vecchio DO-D, Han E, Silva PM, Galaverni M, Fan Z,  
27 Marx P, Lorente-Galdos B, et al. 2014. Genome Sequencing Highlights the Dynamic  
28 Early History of Dogs. *PLOS Genet* 10:e1004016.
- 29 Fu Q, Posth C, Hajdinjak M, Petr M, Mallick S, Fernandes D, Furtwängler A, Haak W, Meyer  
30 M, Mittnik A, et al. 2016. The genetic history of Ice Age Europe. *Nature* 534:200–  
31 205.
- 32 Geffen E, Anderson MJ, Wayne RK. 2004. Climate and habitat barriers to dispersal in the  
33 highly mobile grey wolf. *Molecular Ecology* 13:2481–2490.
- 34 Germonpré M, Fedorov S, Danilov P, Galeta P, Jimenez E-L, Sablin M, Losey RJ. 2017.  
35 Palaeolithic and prehistoric dogs and Pleistocene wolves from Yakutia: Identification  
36 of isolated skulls. *Journal of Archaeological Science* 78:1–19.
- 37 Germonpré M, Hämäläinen R. 2007. Fossil Bear Bones in the Belgian Upper Paleolithic: The  
38 Possibility of a Proto Bear-Ceremonialism. *Arctic Anthropology* 44:1–30.

- 1 Germonpré M, Lázničková-Galetová M, Losey RJ, Rääkkönen J, Sablin MV. 2015. Large canids  
2 at the Gravettian Předmostí site, the Czech Republic: The mandible. *Quaternary*  
3 *International* 359–360:261–279.
- 4 Germonpré M, Lázničková-Galetová M, Sablin MV. 2012. Palaeolithic dog skulls at the  
5 Gravettian Předmostí site, the Czech Republic. *Journal of Archaeological Science*  
6 39:184–202.
- 7 Germonpré M, Sablin MV, Stevens RE, Hedges REM, Hofreiter M, Stiller M, Després VR.  
8 2009. Fossil dogs and wolves from Palaeolithic sites in Belgium, the Ukraine and  
9 Russia: osteometry, ancient DNA and stable isotopes. *Journal of Archaeological*  
10 *Science* 36:473–490.
- 11 Godinho R, Llaneza L, Blanco JC, Lopes S, Álvares F, García EJ, Palacios V, Cortés Y, Tategón J,  
12 Ferrand N. 2011. Genetic evidence for multiple events of hybridization between  
13 wolves and domestic dogs in the Iberian Peninsula. *Molecular Ecology* 20:5154–  
14 5166.
- 15 Groucutt HS, Petraglia MD, Bailey G, Scerri EML, Parton A, Clark-Balzan L, Jennings RP, Lewis  
16 L, Blinkhorn J, Drake NA, et al. 2015. Rethinking the dispersal of *Homo sapiens* out of  
17 Africa. *Evol. Anthropol.* 24:149–164.
- 18 Hofreiter M, Stewart J. 2009. Ecological Change, Range Fluctuations and Population  
19 Dynamics during the Pleistocene. *Current Biology* 19:R584–R594.
- 20 Hopkins D, Matthews J, Schweger C. 1982. *Paleoecology of Beringia*. 1st ed. Academic Press
- 21 Kimura M, Weiss GH. 1964. The Stepping Stone Model of Population Structure and the  
22 Decrease of Genetic Correlation with Distance. *Genetics* 49:561–576.
- 23 Kingman JFC. 1982. The coalescent. *Stochastic Processes and their Applications* 13:235–248.
- 24 Koblmüller S, Vilà C, Lorente-Galdos B, Dabad M, Ramirez O, Marques-Bonet T, Wayne RK,  
25 Leonard JA. 2016. Whole mitochondrial genomes illuminate ancient intercontinental  
26 dispersals of grey wolves (*Canis lupus*). *J. Biogeogr.* 43:1728–1738.
- 27 Kuzmina IE, Sablin MV. 1993. Pozdnepleistotsenovyi pesets verhnei Desny. In: *Materiali po*  
28 *mezozoickoi i kainozoickoi istorii nazemnykh pozvonochnykh. Trudy* 17  
29 *Zoologicheskogo Instituta RAN* 249. p. 93–104.
- 30 Lanfear R, Calcott B, Ho SYW, Guindon S. 2012. PartitionFinder: Combined Selection of  
31 Partitioning Schemes and Substitution Models for Phylogenetic Analyses. *Mol Biol*  
32 *Evol* 29:1695–1701.
- 33 Larkin MA, Blackshields G, Brown NP, Chenna R, McGettigan PA, McWilliam H, Valentin F,  
34 Wallace IM, Wilm A, Lopez R, et al. 2007. Clustal W and Clustal X version 2.0.  
35 *Bioinformatics* 23:2947–2948.
- 36 Larson G, Karlsson EK, Perri A, Webster MT, Ho SYW, Peters J, Stahl PW, Piper PJ, Lingaas F,  
37 Fredholm M, et al. 2012. Rethinking dog domestication by integrating genetics,  
38 archeology, and biogeography. *PNAS* 109:8878–8883.
- 39 Leonard JA. 2015. Ecology drives evolution in grey wolves. *Evol Ecol Res* 16:461–473.

- 1 Leonard JA, Vilà C, Fox-Dobbs K, Koch PL, Wayne RK, Van Valkenburgh B. 2007. Megafaunal  
2 Extinctions and the Disappearance of a Specialized Wolf Ecomorph. *Current Biology*  
3 17:1146–1150.
- 4 Lister AM, Stuart AJ. 2008. The impact of climate change on large mammal distribution and  
5 extinction: Evidence from the last glacial/interglacial transition. *Comptes Rendus*  
6 *Geoscience* 340:615–620.
- 7 Loog L, Lahr MM, Kovacevic M, Manica A, Eriksson A, Thomas MG. 2017. Estimating mobility  
8 using sparse data: Application to human genetic variation. *PNAS*:201703642.
- 9 Lorenzen ED, Nogués-Bravo D, Orlando L, Weinstock J, Binladen J, Marske KA, Ugan A,  
10 Borregaard MK, Gilbert MTP, Nielsen R, et al. 2011. Species-specific responses of  
11 Late Quaternary megafauna to climate and humans. *Nature* 479:359–364.
- 12 Lucchini V, Galov A, Randi E. 2004. Evidence of genetic distinction and long-term population  
13 decline in wolves (*Canis lupus*) in the Italian Apennines. *Molecular Ecology* 13:523–  
14 536.
- 15 Mazet O, Rodríguez W, Chikhi L. 2015. Demographic inference using genetic data from a  
16 single individual: Separating population size variation from population structure.  
17 *Theoretical Population Biology* 104:46–58.
- 18 Mazet O, Rodríguez W, Grusea S, Boitard S, Chikhi L. 2016. On the importance of being  
19 structured: instantaneous coalescence rates and human evolution—lessons for  
20 ancestral population size inference? *Heredity* 116:362–371.
- 21 Morey DF. 2014. In search of Paleolithic dogs: a quest with mixed results. *Journal of*  
22 *Archaeological Science* 52:300–307.
- 23 Münzel SC, Conard NJ. 2004. Change and continuity in subsistence during the Middle and  
24 Upper Palaeolithic in the Ach Valley of Swabia (south-west Germany). *Int. J.*  
25 *Osteoarchaeol.* 14:225–243.
- 26 Nielsen R, Beaumont MA. 2009. Statistical inferences in phylogeography. *Molecular Ecology*  
27 18:1034–1047.
- 28 O’Keefe FR, Meachen J, Fet EV, Brannick A. 2013. Ecological determinants of clinal  
29 morphological variation in the cranium of the North American gray wolf. *J Mammal*  
30 94:1223–1236.
- 31 Palkopoulou E, Dalén L, Lister AM, Vartanyan S, Sablin M, Sher A, Edmark VN, Brandström  
32 MD, Germonpré M, Barnes I, et al. 2013. Holarctic genetic structure and range  
33 dynamics in the woolly mammoth. *Proc. R. Soc. B* 280:20131910.
- 34 Paradis E, Claude J, Strimmer K. 2004. APE: Analyses of Phylogenetics and Evolution in R  
35 language. *Bioinformatics* 20:289–290.
- 36 Perri A. 2016. A wolf in dog’s clothing: Initial dog domestication and Pleistocene wolf  
37 variation. *Journal of Archaeological Science* 68:1–4.

- 1 Pilot M, Jedrzejewski W, Branicki W, Sidorovich VE, Jedrzejewska B, Stachura K, Funk SM.  
2 2006. Ecological factors influence population genetic structure of European grey  
3 wolves. *Molecular Ecology* 15:4533–4553.
- 4 Posth C, Renaud G, Mittnik A, Drucker DG, Rougier H, Cupillard C, Valentin F, Thevenet C,  
5 Furtwängler A, Wißing C, et al. 2016. Pleistocene Mitochondrial Genomes Suggest a  
6 Single Major Dispersal of Non-Africans and a Late Glacial Population Turnover in  
7 Europe. *Current Biology* 26:827–833.
- 8 Puzachenko AY, Markova AK. 2016. Diversity dynamics of large- and medium-sized  
9 mammals in the Late Pleistocene and the Holocene on the East European Plain:  
10 Systems approach. *Quaternary International* [Internet]. Available from:  
11 <http://www.sciencedirect.com/science/article/pii/S1040618215007077>
- 12 Raghavan M, Steinrücken M, Harris K, Schiffels S, Rasmussen S, DeGiorgio M, Albrechtsen A,  
13 Valdiosera C, Ávila-Arcos MC, Malaspina A-S, et al. 2015. Genomic evidence for the  
14 Pleistocene and recent population history of Native Americans. *Science*:aab3884.
- 15 Rambaut A. 2000. Estimating the rate of molecular evolution: incorporating non-  
16 contemporaneous sequences into maximum likelihood phylogenies. *Bioinformatics*  
17 16:395–399.
- 18 Rieux A, Eriksson A, Li M, Sobkowiak B, Weinert LA, Warmuth V, Ruiz-Linares A, Manica A,  
19 Balloux F. 2014. Improved Calibration of the Human Mitochondrial Clock Using  
20 Ancient Genomes. *Mol Biol Evol* 31:2780–2792.
- 21 Sablin Mikhail V, Khlopachev Gennady A. 2002. The Earliest Ice Age Dogs: Evidence from  
22 Eliseevichi 1. *Current Anthropology* 43:795–799.
- 23 Sharma DK, Maldonado JE, Jhala YV, Fleischer RC. 2004. Ancient wolf lineages in India.  
24 *Proceedings of the Royal Society of London B: Biological Sciences* 271:S1–S4.
- 25 Sinnott R. 1984. Virtues of the Haversine. *Sky and telescope* 68:159.
- 26 Skoglund P, Ersmark E, Palkopoulou E, Dalén L. 2015. Ancient Wolf Genome Reveals an Early  
27 Divergence of Domestic Dog Ancestors and Admixture into High-Latitude Breeds.  
28 *Current Biology* 25:1515–1519.
- 29 Sotnikova M, Rook L. 2010. Dispersal of the Canini (Mammalia, Canidae: Caninae) across  
30 Eurasia during the Late Miocene to Early Pleistocene. *Quaternary International*  
31 212:86–97.
- 32 Stuart AJ, Kosintsev PA, Higham TFG, Lister AM. 2004. Pleistocene to Holocene extinction  
33 dynamics in giant deer and woolly mammoth. *Nature* 431:684–689.
- 34 Thalmann O, Shapiro B, Cui P, Schuenemann VJ, Sawyer SK, Greenfield DL, Germonpré MB,  
35 Sablin MV, López-Giráldez F, Domingo-Roura X, et al. 2013. Complete Mitochondrial  
36 Genomes of Ancient Canids Suggest a European Origin of Domestic Dogs. *Science*  
37 342:871–874.
- 38 Verardi A, Lucchini V, Randi E. 2006. Detecting introgressive hybridization between free-  
39 ranging domestic dogs and wild wolves (*Canis lupus*) by admixture linkage  
40 disequilibrium analysis. *Molecular Ecology* 15:2845–2855.

- 1 Wang G-D, Zhai W, Yang H-C, Wang L, Zhong L, Liu Y-H, Fan R-X, Yin T-T, Zhu C-L, Poyarkov  
2 AD, et al. 2016. Out of southern East Asia: the natural history of domestic dogs  
3 across the world. *Cell Research* 26:21–33.
- 4 Warmuth V, Eriksson A, Bower MA, Barker G, Barrett E, Hanks BK, Li S, Lomitashvili D, Ochir-  
5 Goryaeva M, Sizonov GV, et al. 2012. Reconstructing the origin and spread of horse  
6 domestication in the Eurasian steppe. *PNAS* 109:8202–8206.
- 7 Wegmann D, Leuenberger C, Neuenschwander S, Excoffier L. 2010. ABCtoolbox: a versatile  
8 toolkit for approximate Bayesian computations. *BMC Bioinformatics* 11:116.
- 9